JOBNAME: JTECH 00#00 2016 PAGE: 1 SESS: 8 OUTPUT: Tue May 10 19:24:15 2016 Total No. of Pages: 8
/ams/jtech/0/jtechD160047

Relating Wind and Stress under Tropical Cyclones with Scatterometer

W. TIMOTHY LIU AND WENQING TANG

Jet Propulsion Laboratory, California Institute of Technology, Pasadena, California

(Manuscript received 16 February 2016, in final form 12 April 2016)

AU1

ABSTRACT

Ocean surface stress, the turbulent transport of momentum, is largely derived from wind through a drag coefficient. In tropical cyclones (TCs), scatterometers have difficulty measuring strong wind and there is large uncertainty in the drag coefficient. This study postulates that the microwave backscatter from ocean surface roughness, which is in equilibrium with local stress, does not distinguish between weather systems. The reduced sensitivity of scatterometer wind retrieval algorithms under the strong wind is an air–sea interaction problem that is caused by a change in the behavior of the drag coefficient rather than a sensor problem. Under this assumption, a stress retrieval algorithm developed over a moderate wind range to retrieve stress under the strong winds of TCs ~~is applied~~ is applied. Over a moderate wind range, the abundant wind measurements and the more established drag coefficient value allow for sufficient stress data to be computed from wind to develop a stress retrieval algorithm for the scatterometer. Using 0.9 million coincident stress and wind pairs, the study shows that the drag coefficient decreases with wind speed at a much steeper rate than previously revealed, for wind speeds over 25 m s^{-1}. The result implies that the ocean applies less drag to inhibit TC intensification, and that TCs cause less ocean mixing and surface cooling than previous studies indicated.

1. Drag coefficient

Wind is air in motion, and stress (τ) is the turbulent transport of momentum between the ocean and the atmosphere. While the strong wind of a tropical cyclone (TC) causes destruction at landfall, it is the surface stress that drags down the TC. ~~In our study,~~ There was almost no stress measurement except in dedicated field campaigns, and the stress estimates ~~we used~~ were almost entirely derived from wind measurements. A drag coefficient (C_D) is used to derive τ from wind (U) at a reference height, and it is defined as

$$\tau = \rho C_D (U - U_S)^2, \quad (1)$$

where U_s is the surface current and ρ is the air density. Wind and stress are vector quantities but only their magnitudes are considered in this study. Although we include U_s in Eq. (1), it is usually ignored because its magnitude is small compared with wind. Similar coefficients C_H and C_E are used to related turbulent fluxes of sensible and latent heat to temperature and humidity differences, respectively (see Liu et al. 1979 for a review).

The drag coefficient has been well studied and derived largely in field campaigns. For a moderate range of wind speed, the drag coefficient is found to increase with wind speed. Secondary factors (Geernaert et al. 1986; Donelan 1990; Smith et al. 1992), such as sea states, swell, and spray from breaking waves, together with the stability effects (the balance between wind shear and buoyancy) are not included, and they contribute to the uncertainties of the C_D.

Liu et al. (1979) first postulated that, in a rough sea, under a moderate range of winds (between 3 and 20 m s^{-1}), C_H and C_E do not increase with wind speed because of molecular constraint at the interface, while C_D may still increase because momentum is transported by form drag over the waves. Emanuel (1995) argued, from theoretical and numerical model results, that the scenario of Liu et al. (1979) could not hold at the strong wind regime of a TC. To attain the wind strength of a TC, the energy dissipated by drag could not keep increasing while the energy fed by sensible and latent heat does not increase with wind speed. His argument puts a limit on the increase of C_D as a function of wind speed.

The postulation that the increase of C_D with wind speed will level off or decrease at TC-scale winds was

Corresponding author address: W. Timothy Liu, Jet Propulsion Laboratory, California Institute of Technology, M/S 300-323, 4800 Oak Grove Dr., Pasadena, CA 91109.
E-mail: w.t.liu@jpl.nasa.gov

DOI: 10.1175/JTECH-D-16-0047.1

JOBNAME: JTECH 00#00 2016 PAGE: 2 SESS: 8 OUTPUT: Tue May 10 19:24:15 2016 Total No. of Pages: 8
/ams/jtech/0/jtechD160047

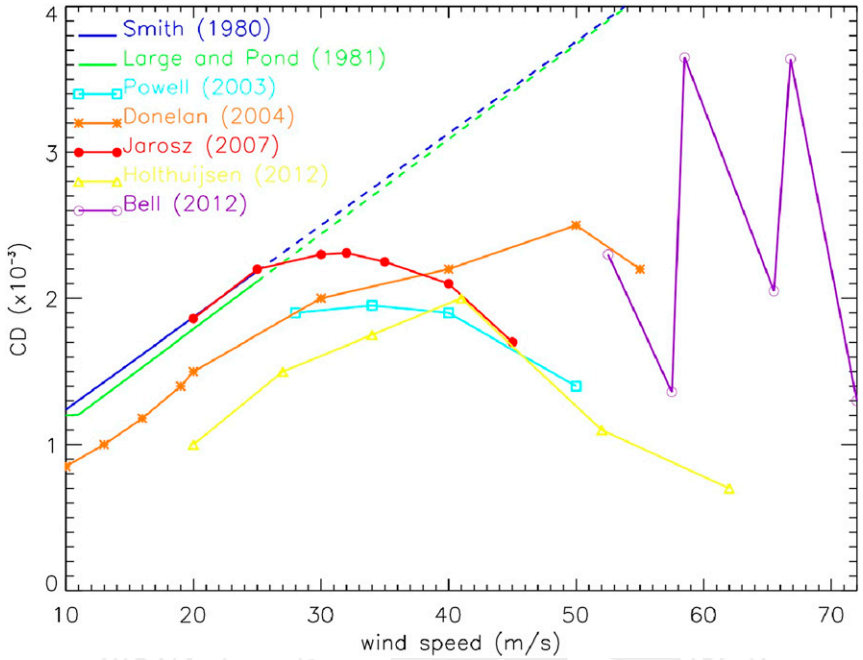

FIG. 1. Drag coefficients as a function of wind speed. Broken lines are extrapolations.

supported by the results of many subsequent studies. In Fig. 1, examples of C_D for TC as a function of wind speed are shown together with the extension of C_D established for moderate winds (Large and Pond 1981; Smith 1980). Donelan et al. (2004) measured stress in a laboratory. Powell et al. (2003) derived stress from the gradient of a wind profile measured by dropsondes assuming a logarithmic distribution. French et al. (2007) measured stress using an eddy correlation method in an aircraft, but not in very high winds (not shown). Recently, Jarosz et al. (2007) estimated stress from current measurements, Holthuijsen et al. (2012) also addressed wave breaking, and Bell et al. (2012) based their estimates on angular momentum balance. Soloviev et al. (2014) gives a more recent review of C_D values and postulations on its behavior at high winds. Despite all the innovative stress estimates of TCs, the large spread of the values in the figure shows clearly the unsatisfactory stage of our present knowledge.

2. Scatterometer

The scatterometer is the most established space-based instrument to measure ocean surface stress vector (Liu 2002; Liu and Xie 2006). It sends microwave pulses to the earth's surface and measures the power backscattered from the surface roughness. Over the ocean, the surface roughness is largely due to the small centimeter-length waves (including capillary waves), which are believed to be in equilibrium with the surface stress. The initial geophysical model functions relate measured normalized radar cross section σ_o to the frictional velocity $U_* = (\tau/\rho)^{1/2}$, representing kinematic stress. The expression is

$$\sigma_o = f(U_*, \chi, \theta, p), \tag{2}$$

where χ is the relative azimuth angle between the plane of incidence of the radar beam and the stress direction, θ is the incidence angle (relative to nadir), and p represents the polarization (e.g., Jones and Schroeder 1978). The data products of the first operational *Seasat* scatterometer were validated against measured stress (Liu and Large 1981). Because the public is more familiar with wind than stress, and there are more wind measurements than stress measurements for calibration and validation, the equivalent neutral wind U_N has been used as the geophysical product. Wind U_N, by definition, has an unambiguous relation with stress, while the relation between actual wind and stress depends also on atmospheric density stratification [see Liu et al. (2010) and Liu and Xie (2014) for further explanation]. Under the strong wind of a TC, wind shear dominates over buoyancy in turbulence generation, and U_N is close to the actual wind. Nonetheless, there were recent attempts on stress retrieval algorithms (e.g., Weissman and Graber 1999). QuikSCAT has a conical scanning pencil-beam antenna operating at 13.4 GHz (Ku band) at a fixed incidence angle of about 46° and 54° for

JOBNAME: JTECH 00#00 2016 PAGE: 3 SESS: 8 OUTPUT: Tue May 10 19:24:16 2016 Total No. of Pages: 8
/ams/jtech/0/jtechD160047

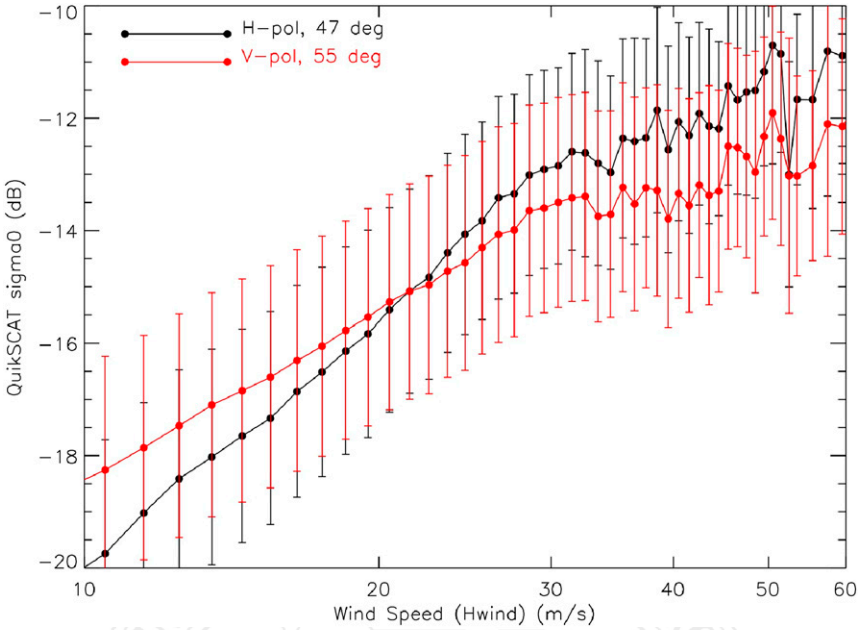

FIG. 2. Backscatter coefficient for two beams (identified by their polarization and incident angles) measured by QuikSCAT collocated with H*wind along all reported hurricanes paths in the North Atlantic from 2005 to 2008. QuikSCAT data with more than 10% chance of rainfall are excluded.

horizontal polarization (H-pol; inner beam) and vertical polarization (V-pol; outer beam), respectively.

The difficulty of retrieving strong winds from the scatterometer is obvious in Fig. 2. Data from North Atlantic hurricanes in four seasons (2005–08), excluding those with over 10% chance of rain, were examined. QuikSCAT σ_o from the two beams are plotted against collocated Hurricane Research Division Real-time Hurricane Wind Analysis System (H*wind) speed, at a bin size of $1\,\mathrm{m\,s^{-1}}$. H*wind is described in section 4. Figure 2 shows that, in moderate winds ($U < 30\,\mathrm{m\,s^{-1}}$), the logarithm of σ_o (dB) increases almost linearly with the logarithm of wind speed. At strong winds ($U > 30\,\mathrm{m\,s^{-1}}$), however, σ_o increases at a much slower rate with increasing wind speed. The European Advanced Scatterometer, measuring at C band, observes similar saturation. Such high wind saturation has also been observed from aircraft flying over TCs (e.g., Donnelly et al. 1999). When the model function developed over the moderate wind range is applied to the strong winds, an underestimation of wind speed results. Strong efforts have been made to adjust the model function (slope in Fig. 2) in strong winds, but there are not sufficient in situ measurements available to give credible results. The regressions for the two datasets cross each other at $U = 20\,\mathrm{m\,s^{-1}}$, showing different sensitivities for different polarizations and incidence angles. The variations caused by the change in azimuth angle should be a major part of the error bars. The azimuth dependence was clearly illustrated by Ebuchi (2000). There were efforts to find a remote sensing solution—that is, to find the right channel (a combination of polarization, frequency, incidence angle)—that would be more sensitive to the increase of strong winds (e.g., Fernandez et al. 2006).

3. Hypothesis

We assume that there is no distinct physics governing radar backscatter from ocean surface for different weather phenomena, including TCs [Eq. (2)]. The algorithm that relates σ_o to surface roughness was initially developed based on theory, artificial waves, and stationary roughness, independent of surface aerodynamics (e.g., Wright 1968; Brown 1978) and did not consider weather change. The general relation should apply with or without TCs. The formation of surface roughness, with close bond to stress, is an air–sea interaction problem that may depend on weather. The changes in the wind retrieval algorithm under a TC, as shown in section 2, is not a remote sensing problem but an air–sea interaction problem caused by flow separation as manifested in the change of the C_D in TCs. Based on this hypothesis, we can use a stress retrieval algorithm developed under a moderate range of wind speeds

JOBNAME: JTECH 00#00 2016 PAGE: 4 SESS: 8 OUTPUT: Tue May 10 19:24:16 2016 Total No. of Pages: 8
/ams/jtech/0/jtechD160047

TABLE 1. List of the number of tropical storms and collocated QuikSCAT backscatter snapshots along the best tracks from storms during the period 2005–08 in the North Atlantic, northwestern Pacific, and eastern Pacific. Combining three basins in 4 years, there were a total of 236 storms and 4475 snapshots.

	2005		2006		2007		2008	
	Storm	Snapshot	Storm	Snapshot	Storm	Snapshot	Storm	Snapshot
North Atlantic	28	577	10	273	15	234	16	329
Northwest Pacific	25	509	26	522	27	456	27	463
East Pacific	15	260	19	336	11	196	17	320
Total	68	1346	55	1131	53	886	60	1112

to retrieve stress under the strong winds of TCs. With an unprecedented large number of stress data retrieved from the scatterometer, the variation of stress and C_D under TCs can be reexamined.

4. Data

QuikSCAT level 2A σ_o data (PODAAC 2007) were reprocessed to produce the averaged σ_o for each wind vector cell (WVC) corresponding to H-pol and V-pol for forward and backward looks, respectively. We compiled two sets of wind data. One set was for moderate winds with $U < 25\,\mathrm{m\,s^{-1}}$, to derive stress for construction of the retrieval algorithm; they are entirely from WindSat measurements. The other set was for strong winds with $U > 20\,\mathrm{m\,s^{-1}}$, for evaluating the C_D; they were from three sets of observations: WindSat, H*Wind, and dropsondes. Both moderate and strong wind datasets were collocated with QuikSCAT σ_o over TC tracks.

WindSat is a polarimetric radiometer that was launched in 2003; it is capable of measuring wind vectors (Gaiser et al. 2004). Only satellite sensors can provide sufficiently large sets of measurements collocated with σ_o to cover variations of azimuth angles, and those associated with secondary factors (section 1), to mitigate aliasing in the bin averages, upon which we perform our analysis. Windsat had the closest overlap with QuikSCAT in coverage among all the relevant sensors. Although we encountered initial application difficulties (e.g., Liu et al. 2004) and known deficiencies, the reprocessed data have provided a consistent target to calibrate various wind speed–measuring sensors for more than a decade at Remote Sensing Systems (Ricciardulli and Wentz 2015). However, very few data are above $35\,\mathrm{m\,s^{-1}}$.

For strong wind measurements in TCs, we used about 9000 dropsondes deployed from airplanes that were tracked by a global positioning system collected during several tropical cyclone campaigns during 2007–10. Chou et al. (2013) performed quality control and provided the surface wind data to us. For collocation, QuikSCAT data were averaged within 25-km grids surrounding the dropsonde locations.

Strong winds between 35 and $45\,\mathrm{m\,s^{-1}}$ come largely from the operational product of the Hurricane Research Division real-time hurricane wind analysis system H*wind (Powell et al. 1998). The data were produced from surface winds within a time window of TC passes from various sources, projected to a level of 10 m, and linearly interpolated to complete a wind field representative of the entire cyclone. H*wind data cover only a small area around the storm center (SC) in the North Atlantic and are generated at irregular times. We had to increase the collocation time window to 6 hours.

The Joint Typhoon Warning Center and the National Hurricane Center report locations of an SC every 6 h. If a QuikSCAT swath passes over any SC, then a subset of σ_o within 1000 km from the SC is created on a 25 km × 25 km grid and is named a "snapshot. Table 1 lists the number of tropical storms and snapshots from 2005 to 2008 extracted from QuikSCAT. A similar procedure is applied to WindSat. Snapshots of data from the two satellites within an hour are used. The dislocations caused by the small time difference between QuikSCAT and Windsat coverage were neglected. The resulting ensemble database contains collocated QuikSCAT σ_o for H-pol and V-pol for forward and afterward looks, respectively, and Windsat wind vectors.

5. Stress algorithm

To develop an algorithm to retrieve stress from σ_o, we first derived a set of stress from wind data under a moderate range of wind speeds in the TCs, where wind measurements in TC coincident with QuikSCAT observations are abundant, and the C_D is more established. We collocated WindSat wind vectors with QuikSCAT σ_o, as described in section 4. The C_D by Large and Pond (1981) was used to derive stress from Windsat winds. The collocated τ and σ_o data are shown in Fig. 3, with four linear regressions of the bin averages in form of $\log_{10}\tau = a + b\sigma_o$, with σ_o in decibels. The coefficients a and b for the two looks for the two beans are listed in the figure. The difference in the regressions between the forward- and backward-looking data is small.

JOBNAME: JTECH 00#00 2016 PAGE: 5 SESS: 8 OUTPUT: Tue May 10 19:24:16 2016 Total No. of Pages: 8
/ams/jtech/0/jtechD160047

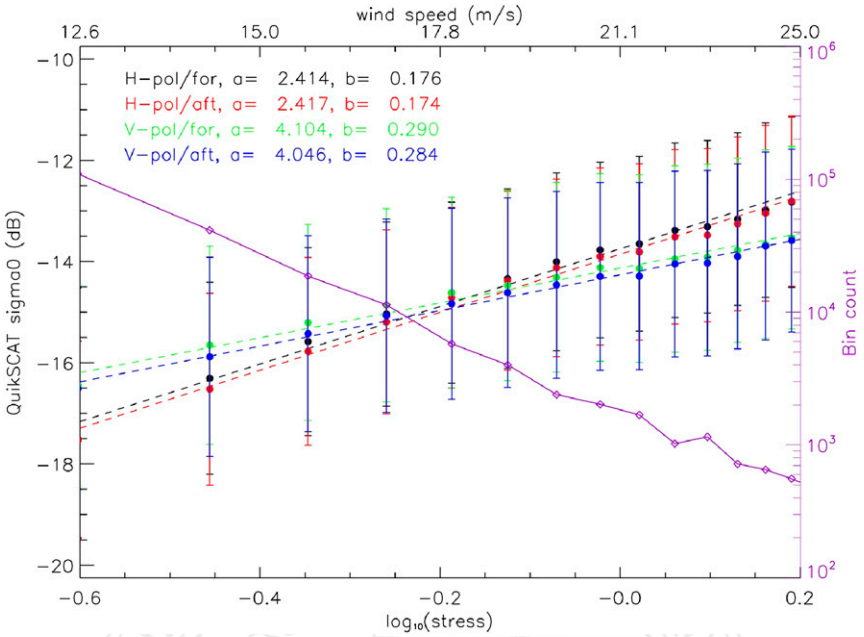

FIG. 3. Backscatter for forward (for) and backward (aft) looks at two beams of horizontal and vertical polarizations, collocated with ocean surface stress, and the linear regressions of the bin averages. The coefficients of the linear regressions are given as a and b. The number of data pairs in each bin is also plotted (purple line). The wind values corresponding to the stress scale are shown on the top of the figure.

The numbers of data in each bin are also plotted. The number decreases from 10 000 to 500 at a range equivalent to wind speed from 12.6 to 25 m s^{-1}. By averaging out the variations caused by directional (azimuth angle) dependence with large amounts of data, we establish relations between mean σ_o and stress. These simple relations allow us to retrieve stress directly from QuikSCAT.

6. Results on stress

Applying the relations shown in Fig. 3, an unprecedented amount of stress was produced from QuikSCAT data, collocated with the high winds above 20 m s^{-1} we assembled by combining WindSat, H*wind, and dropsonde measurements as described in section 3. The data counts for all wind speeds from 20 to 40 m s^{-1} are shown Fig. 4. The total number of collocated pairs of wind and stress are 39 759 and 47 093 for the outer and inner beams, respectively. They vary from 10 000 at 20 m s^{-1}, decrease to 1000 at 30 m s^{-1}, and decrease to 100 at 40 m s^{-1}. There are too few data above 40 m s^{-1} and are not included in our analysis.

The stress in the form of U^* clearly increases with wind speed up to a wind speed of 30 m s^{-1}, and the increase is much slower at a higher wind speed. The same set of collocated stress and wind speed is used to compute the C_D as defined in Eq. (1). They are shown in Fig. 5 as a function of wind speed and compared with some of those shown in Fig. 1. Between 20 and 25 m s^{-1} winds, the C_D from scatterometer stress is enveloped by past values. With wind speed above 25 m s^{-1}, the values of C_D decrease significantly with wind speed at a steeper slope than those of past formulations. A linear regression combining both beams of data is shown. The formulation is

$$C_D = (3.89 - 0.075U) \times 10^{-3}.$$

7. Discussion

This study is not intended to produce a new stress dataset for general applications, but just to demonstrate our postulation that the same stress retrieval algorithm at a moderate range of wind speed may apply under TC conditions, and that the known wind retrieval difficulty is an air–sea interaction problem—not an engineering one. We focus only on the mean signal of the backscatter from two beams, assuming the variations in azimuth angle could be averaged out. We do not find significant difference between forward- and backward-looking data. In this simple study, we also bury the secondary effects of bulk parameterization in the error bars of the bin averages.

JOBNAME: JTECH 00#00 2016 PAGE: 6 SESS: 8 OUTPUT: Tue May 10 19:24:16 2016 Total No. of Pages: 8
/ams/jtech/0/jtechD160047

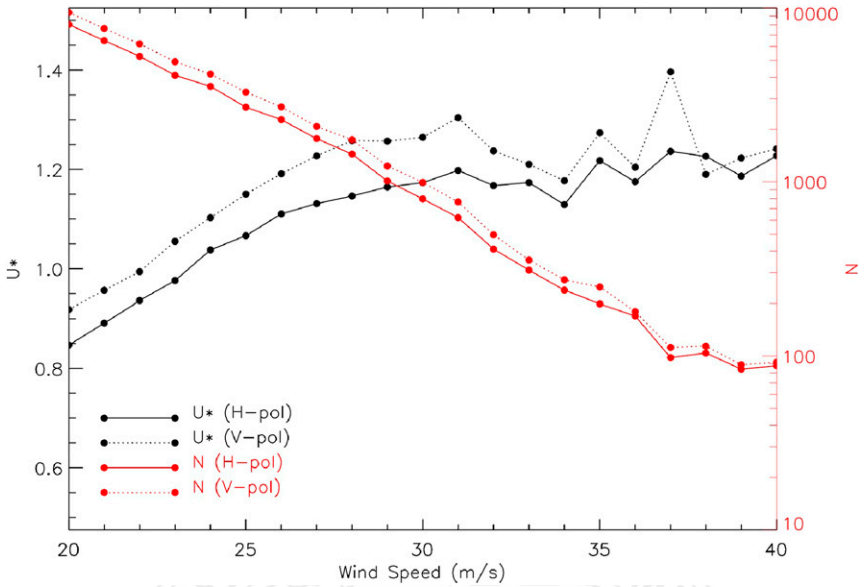

FIG. 4. Friction velocity retrieved from QuikSCAT for two beams as a function of collocated winds. The red lines show the number of data pairs.

The results confirm that the scatterometer is a unique stress rather than a wind sensor; the difference is accentuated under the strong winds of TCs. Over the centimeter-length surface waves that govern the Ku-band backscatter, stress increases at much slower rate, and the C_D decreases at a much faster rate, with increasing wind speed, than demonstrated in past studies that were limited by stress measurements. Our results imply less drag by the ocean on TCs; the impact on cyclone intensification needs to be assessed (e.g., Moon et al. 2007).

Stress also causes ocean mixing and upwelling that bring up colder water from below and reduces sea

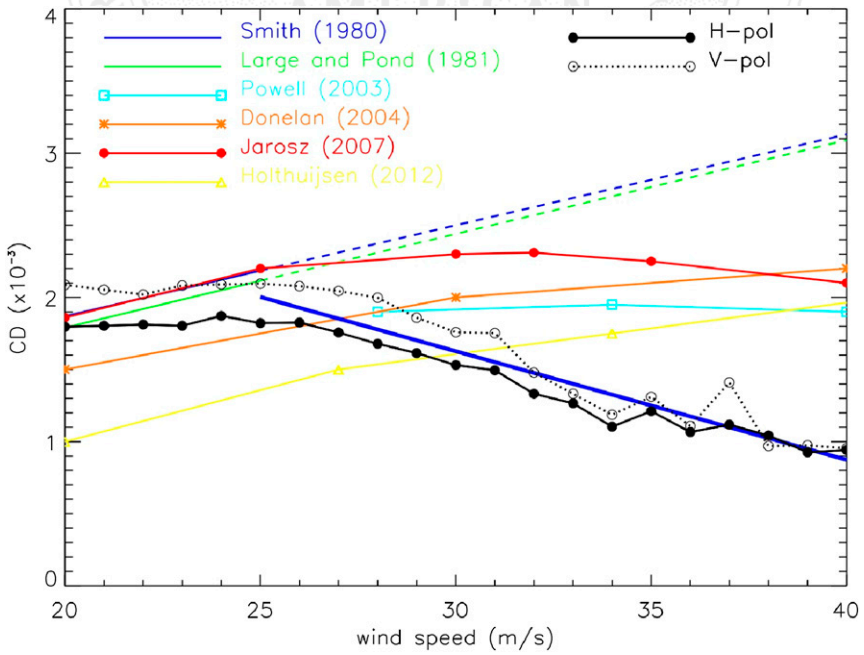

FIG. 5. Drag coefficient as a function of wind speed computed from stress measured by QuikSCAT, with a linear regression of the combined bin averages (thick blue line), superimposed onto the drag coefficients of past studies shown on Fig. 1.

surface temperature (e.g., Price 1981; Bender and Ginis 2000; Lin and Chan 2014). The cooling affects sensible and latent heat fluxes. In light of the reduction of the rates of stress increases with wind speed that are commonly used, the assessments of the ocean's feedback and the effect of global warming on TCs (e.g., Huang et al. 2014) need to be reexamined. It will be the challenge of future studies to assess sensor sensitivity to wind and stress directions in TCs. We also need to push spatial resolution to examine any stress gradient around TC eyewalls and the effect of surface wave and current distributions on stress (e.g., Chen et al. 2013).

Acknowledgments. This study was performed at the Jet Propulsion Laboratory, California Institute of Technology, under contract with the National Aeronautics and Space Administration (NASA). It was supported by the Physical Oceanography and Cyclone Global Navigation Satellite System programs of NASA. We are deeply grateful to Kun-Hsuan Chou for providing the dropsonde data and for the advice of I.-I. Lin on typhoon studies. Xiaosu Xie kindly helped us with the data analysis. WindSat data were obtained from Remote Sensing Systems, Inc. Government sponsorship is acknowledged.

REFERENCES

Bell, M. M., M. T. Montgomery, and K. A. Emanuel, 2012: Air–sea enthalpy and momentum exchange at major hurricane wind speeds observed during CBLAST. *J. Atmos. Sci.*, **69**, 3197–3222, doi:10.1175/JAS-D-11-0276.1.

Bender, M. A., and I. Ginis, 2000: Real-case simulations of hurricane–ocean interaction using a high-resolution coupled model: Effects on hurricane intensity. *Mon. Wea. Rev.*, **128**, 917–946, doi:10.1175/1520-0493(2000)128<0917:RCSOHO>2.0.CO;2.

Brown, G. S., 1978: Backscattering from a Gaussian-distributed perfectly conducting rough surface. *IEE Trans. Antennas Propag.*, **26**, 472–482, doi:10.1109/TAP.1978.1141854.

Chen, S. S., W. Zhao, M. A. Donelan, and H. L. Tolman, 2013: Directional wind–wave coupling in fully coupled atmosphere–wave–ocean models: Results from CBLAST-Hurricane. *J. Atmos. Sci.*, **70**, 3198–3214, doi:10.1175/JAS-D-12-0157.1.

Chou, K.-H., C.-C. Wu, and S.-Z. Lin, 2013: Assessment of the ASCAT wind error characteristics by global dropwindsonde observations. *J. Geophys. Res. Atmos.*, **118**, 9011–9021, doi:10.1002/jgrd.50724.

Donelan, M. A., 1990: Air-sea interaction. *Ocean Engineering Science, Parts A and B*, B. LeMehaute and D. M. Hanes, Eds., The Sea—Ideas and Observations on Progress in the Study of the Seas, Vol. 9, Wiley & Sons, 339–292.

——, B. K. Haus, N. Reul, W. J. Plant, M. Stiassnie, H. C. Graber, O. B. Brown, and E. S. Saltzman, 2004: On the limiting aerodynamic roughness of the ocean in very strong winds. *Geophys. Res. Lett.*, **31**, L18306, doi:10.1029/2004GL019460.

Donnelly, W., J. Carswell, R. McIntosh, P. S. Chang, J. Wilkerson, P. Black, and F. Marks, 1999: Revised ocean backscatter models at C and Ku band under high-wind conditions. *J. Geophys. Res.*, **104**, 11 485–11 497, doi:10.1029/1998JC900030.

Ebuchi, N., 2000: Evaluation of NSCAT-2 wind vectors by using statistical distribution of wind speeds and directions. *J. Oceanogr.*, **56**, 161–172, doi:10.1023/A:1011183029009.

Emanuel, K., 1995: Sensitivity of tropical cyclones to surface exchange coefficients and a revised steady-state model incorporating eye dynamics. *J. Atmos. Sci.*, **52**, 3969–3976, doi:10.1175/1520-0469(1995)052<3969:SOTCTS>2.0.CO;2.

Fernandez, D. E., J. R. Carswell, S. Frasier, P. S. Chang, P. G. Black, and F. D. Marks, 2006: Dual-polarized C- and Ku-band ocean backscatter response to hurricane-force winds. *J. Geophys. Res.*, **111**, C08013, doi:10.1029/2005JC003048.

French, J. R., W. M. Drennan, J. A. Zhang, and P. G. Black, 2007: Turbulent fluxes in the hurricane boundary layer. Part I: Momentum flux. *J. Atmos. Sci.*, **64**, 1089–1102, doi:10.1175/JAS3887.1.

Gaiser, P. W., and Coauthors, 2004: The WindSat spaceborne polarimetric microwave radiometer: Sensor description and early orbit performance. *IEEE Trans. Geosci. Remote Sens.*, **42**, 2347–2361, doi:10.1109/TGRS.2004.836867.

Geernaert, G. L., K. B. Katsaros, and K. Richter, 1986: Variation of the drag coefficient and its dependence on sea state. *J. Geophys. Res.*, **91**, 7667–7679, doi:10.1029/JC091iC06p07667.

Holthuijsen, L. H., M. D. Powell, and J. D. Pietrzak, 2012: Wind and waves in extreme hurricanes. *J. Geophys. Res.*, **117**, C09003, doi:10.1029/2012JC007983.

Huang, P., I.-I. Lin, C. Chou, and R.-H. Huang, 2014: Change in ocean subsurface environment to suppress tropical cyclone intensification under global warming. *Nat. Commun.*, **6**, 7188, doi:10.1038/ncomms8188.

Jarosz, E., D. A. Mitchell, D. W. Wang, and W. J. Teague, 2007: Bottom-up determination of air-sea momentum exchange under a major tropical cyclone. *Science*, **315**, 1707–1709, doi:10.1126/science.1136466.

Jones, W. L., and L. C. Schroeder, 1978: Radar backscatter from the ocean: Dependence on surface friction velocity. *Bound.-Layer Meteor.*, **13**, 133–149, doi:10.1007/BF00913867.

Large, W. G., and S. Pond, 1981: Open ocean momentum flux measurements in moderate to strong winds. *J. Phys. Oceanogr.*, **11**, 324–336, doi:10.1175/1520-0485(1981)011<0324:OOMFMI>2.0.CO;2.

Lin, I.-I., and J. C. L. Chan, 2014: Recent decrease in typhoon destructive potential and global warming implications. *Nat. Commun.*, **6**, 7182, doi:10.1038/ncomms8182.

Liu, W. T., 2002: Progress in scatterometer application. *J. Oceanogr.*, **58**, 121–136, doi:10.1023/A:1015832919110.

——, and W. G. Large, 1981: Determination of surface stress by Seasat-SASS: A case study with JASIN data. *J. Phys. Oceanogr.*, **11**, 1603–1611, doi:10.1175/1520-0485(1981)011<1603:DOSSBS>2.0.CO;2.

——, and X. Xie, 2006: Measuring ocean surface wind from space. *Remote Sensing of the Marine Environment*, 3rd ed. J. Gower, Ed., Manual of Remote Sensing, Vol. 6, American Society of Photogrammetry and Remote Sensing, 149–178.

——, and ——, 2014: Sea surface wind/stress vector. *Encyclopedia of Remote Sensing*, E. Njoku, Ed., Springer-Verlag, 759–767, doi:10.1007/978-0-387-36699-9_168. AU2

——, K. B. Katsaros, and J. A. Businger, 1979: Bulk parameterization of air-sea exchanges of heat and water vapor including the molecular constraints at the interface. *J. Atmos. Sci.*, **36**, 1722–1735, doi:10.1175/1520-0469(1979)036<1722:BPOASE>2.0.CO;2.

——, S.-B. Kim, T. Lee, Y. T. Song, W. Tang, and R. Atlas, 2004: Scientific impacts of wind direction errors. JPL Publ. 04-008, 28 pp. [Available online at http://ntrs.nasa.gov/archive/nasa/casi.ntrs.nasa.gov/20050185098.pdf.]

——, X. Xie, and W. Tang, 2010: Scatterometer's unique capability in measuring ocean surface stress. *Oceanography from Space:*

Revisited, V. Barale, J. F. R. Gower, and L. Alberotanza, Eds., Springer, 93–111.

Moon, I.-J., I. Ginis, T. Hara, and B. Thomas, 2007: A physics-based parameterization of air–sea momentum flux at high wind speeds and its impact on hurricane intensity predictions. *Mon. Wea. Rev.*, **135**, 2869–2878, doi:10.1175/MWR3432.1.

PODAAC, 2007: QuikSCAT science data product user's manual—Overview and geophysical data products. Version 3.0, T. Lungu, Ed., JPL Doc. D-18053, 91 pp. [Available online at ftp://podaac.jpl.nasa.gov/allData/quikscat/L2A/v2/docs/QSUG_v3.pdf.]

Powell, M. D., S. H. Houston, L. R. Amat, and N. Morisseau-Leroy, 1998: The HRD real-time hurricane wind analysis system. *J. Wind Eng. Ind. Aerodyn.*, **77 & 78**, 53–64.

——, P. J. Vickery, and T. A. Reinhold, 2003: Reduced drag coefficient for high wind speeds in tropical cyclones. *Nature*, **422**, 279–283, doi:10.1038/nature01481.

Price, J. F., 1981: Upper ocean response to a hurricane. *J. Phys. Oceanogr.*, **11**, 153–175l, doi:10.1175/1520-0485(1981)011<0153:UORTAH>2.0.CO;2.

Ricciardulli, L., and F. J. Wentz, 2015: A scatterometer geophysical model function for climate-quality winds: QuikSCAT Ku-2011. *J. Atmos. Oceanic Technol.*, **32**, 1829–1846, doi:10.1175/JTECH-D-15-0008.1.

Smith, S. D., 1980: Wind stress and heat flux over the ocean in gale force winds. *J. Phys. Oceanogr.*, **10**, 709–726, doi:10.1175/1520-0485(1980)010<0709:WSAHFO>2.0.CO;2.

——, and Coauthors, 1992: Sea surface wind stress and drag coefficients: The hexos results. *Bound.-Layer Meteor.*, **60**, 109–142, doi:10.1007/BF00122064.

Soloviev, A., R. Lukas, M. Donelan, B. Haus, and I. Ginis, 2014: The air-sea interface and surface stress under tropical cyclones. *Sci. Rep.*, **4**, 5306, doi:10.1038/srep05306.

Weissman, D. E., and H. C. Graber, 1999: Satellite scatterometer studies of ocean surface stress and drag coefficient direct model. *J. Geophys. Res.*, **104**, 11 329–11 335, doi:10.1029/1998JC900117.

Wright, J. W., 1968: A new model for sea clutter. *IEEE Trans. Antennas Propag.*, **16**, 217–233, doi:10.1109/TAP.1968.1139147.